

# Computer Simulation of Microstructure of Particle Sediment

Jong Cheol Kim, Keun Ho Auh and David M. Martin<sup>†</sup>

*Hanyang University, Ceramic Materials Research Institute, Seoul 133-791, Korea*

*<sup>†</sup>Department of Materials Science and Engineering,*

*Iowa State University, Ames, Iowa, 50011, USA*

(Received January 27, 1999)

---

Particle settling behavior was studied by the computer simulation using simultaneous particle condensation and relaxation. This three-dimensional settling algorithm includes the estimation of powder sediment density. Density distribution through the powder sediment was compared and was agreed well with the experimental findings. Settling density depended strongly on the degree of particle relaxation. Sediment strength and isotropy also depended on the degree of particle relaxation. Severe particle bridging was found near sharp corners.

**Key words :** Computer, Simulation, Settle, Particle, Relaxation, Microstructure

---

## I. Introduction

The settling of particles in liquid media and the microstructural characteristics of the resulting sediments are studied frequently because of their great importance in the ceramic processing.<sup>1-5)</sup> There are mainly three forces acting upon a particle in a concentrated suspension: gravitational force, Brownian force and surface force. Settling rates can be determined by plotting the height of the interfacial plane between the concentrated suspension and the supernatant as a function of time.<sup>2)</sup> In the case of very dilute suspensions the settling shows steady decrease in the height of the interface between the slurry and the supernatant. The Richardson and Zaki equation for the group settling rate for uniform, spherical particles is as follows and works well for hard colloidal particles.<sup>3,4)</sup>

$$Q = V_{sa} \epsilon^{4.65} \quad (1)$$

where  $V_{sa}$  is Stokes settling velocity in cm/hr and  $\epsilon$  is a void fraction.

In the case of the intermediate concentrations the settling rate shows steady increase initially and a maximum value. During the early stage of the settling period there is a constant density zone which equals to the density of the initial suspension.

Tiller and Khatib<sup>4)</sup> classified the settling process into induction period, constant density period and variable density period depending on the behavior of settling particles. At high concentration, particles form aggregates and these aggregates form networks with each other. The aggregate networks extend to the walls and bottom of the container. These networks have a mechanical strength and the total volume is supported by underlying material and by shear forces at the walls. In dilute suspensions aggregation leads to the formation discrete

clusters which sediment more or less independently. The clusters form networks above a critical value of particle concentration. This critical concentration depends upon the particle size, particle shape, the strength of aggregation and upon the previous history of the suspension. The network settles or even consolidates depending upon its strength. This gelation was observed even at ~5 volume percent when spherical particles were under rapid perikinetic coagulation.<sup>2)</sup>

Powder settling involves irreversible consolidation of the network under its own weight. The driving force is the compression stress arising from the accumulated weight of the particles. Stress can be transmitted directly throughout the network structure above the gel point. The particulate network has a static strength and it can be characterized by the compressive and the shear yield stress. The static stress at the bottom column is as follows without considering the wall support.

$$P = \Delta \rho g H_0 \phi_0 \quad (2)$$

where  $\Delta \rho$  is the density difference between the particle and the water,  $H_0$  the initial height and  $\phi_0$  the mean volume fraction of solids in the column.

In order for consolidation to occur the static pressure should be greater than the compressive yield stress of the particulate network. Settling affects the microstructure of particle sediments. A dense and uniform particle sediment is important because of its resultant high sintering density and low sintering temperatures. Most of the research on the particle settling has been concentrated on the continuum approaches where it is difficult to consider the properties of individual particles. There are so many complex assumptions in such modeling and it is hard to understand and visualize the individual particle effects. Complex molecular dynamics or Monte Carlo computational approaches<sup>6,7)</sup> to this problem have been tried.

In this research we increased the efficiency of modeling using two simple concepts; condensation and relaxation.<sup>8-10,12)</sup> We developed a program on a PC using FORTRAN 90. The settling process was visually displayed as the computation proceeded to help understand the basic mechanisms of particle sediment.

### 2. Modeling

We used Richardson and Zaki equation for the group settling rate for uniform and spherical particles in equation (1) because this equation works well for hard colloidal particles.<sup>3)</sup> In this equation, settling rate is determined by Stokes settling velocity and the void fraction. We fixed the solid volume concentration in order to compare simulated result with the experimental results reported by Shilling et al.<sup>11)</sup> As a consequence, settling velocity is linearly proportional to the Stokes settling velocity. Settling distance can be calculated by multiplying the settling rate [Q] by time as follows.

$$R(t, \Delta t) = R(t) + [Q] \Delta t \tag{3}$$

where R is the position and t is time.

Particles were settled unit distance at a time and this process was repeated until they touched other particles. Unit settling distance was decided to be a quarter of particle radius to make this computation very efficient. In a monosize particle settling, all particles will settle at the same speed unless particles hit the bottom or other particles. Buscall<sup>2)</sup> reported that particles settle more or less independently in dilute suspensions. The particles may form networks above a certain value of particle concentration where this concentration depends upon particle properties. Buscall et al.<sup>5)</sup> reported that the particles can rearrange as a result of thermal diffusion during sedimentation under weak binding forces. There are several different types of settling behavior in reversibly flocculated systems. In this research, we employed the simplified geometric relaxation concept introduced by Kim and Martin<sup>6)</sup> to represent Buscall's idea. When particles touched other particles, they were assumed to be relaxed by upper particles rotating around lower particles. Fig. 1 shows a general flow chart of the total settling algorithm. The relaxation process starts to run by checking the coordination number (CN) of each particle. If CN is 1, the particle rotates over its neighboring particle in an arbitrary downward direction and if CN is 2, the particle rotates around the line joining the centers of the particles it touches, and when CN is 3, the particle is fixed. Fig. 2 shows how relaxation varies with CN.

### 3. Results and Discussion

For comparison with experimental results the sediment study done by Schilling and Aksay<sup>11)</sup> was used. We used the agglomerate approach<sup>8)</sup> where particle is an agglom-

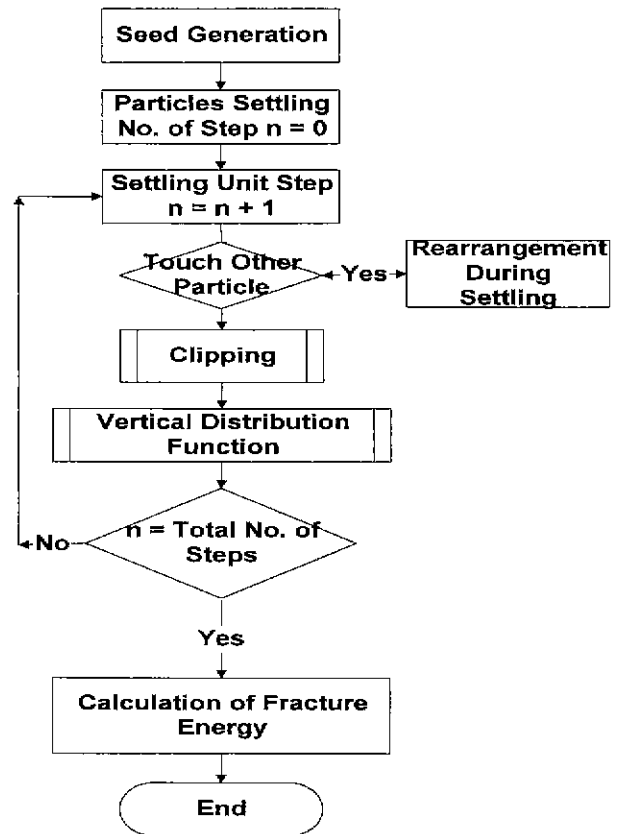


Fig. 1. Flow chart of total settling algorithm.

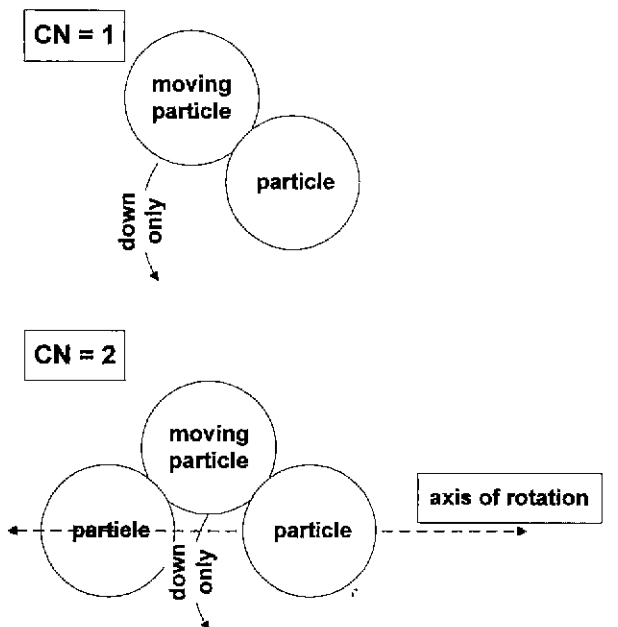
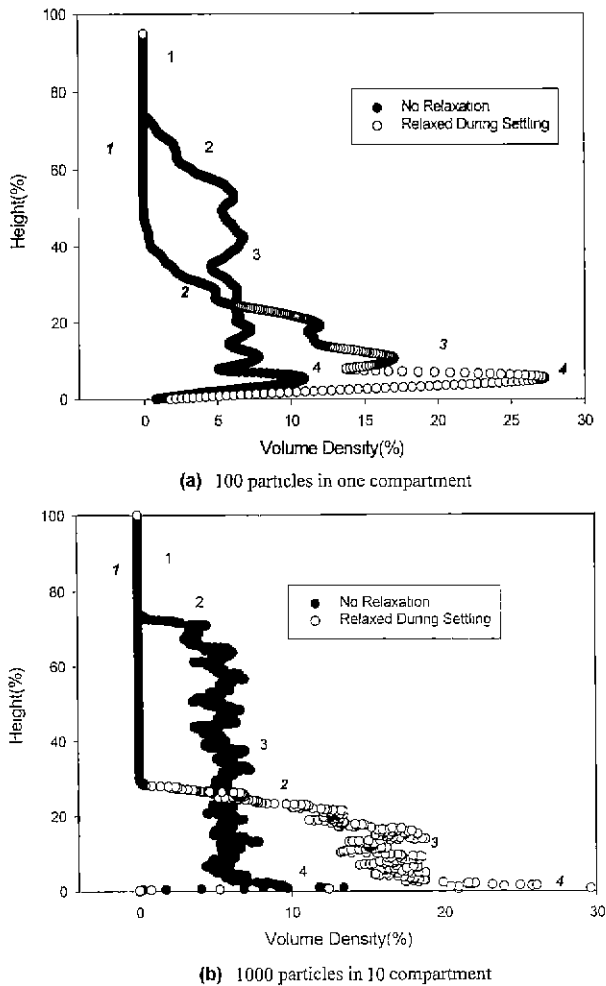


Fig. 2. Relaxation processes with different coordination number.

merate composed of basic particles. The radius of basic particle is 0.4 μ and the size of agglomerate was calculated based on the pore size reported by Schilling and Aksay.<sup>11)</sup> Details in this approximation is explained else-



**Fig. 3.** Vertical density distribution of particle sediments relaxed and not relaxed during settling in a compartment.

where.<sup>12)</sup> Our simulation conditions follow:

Basic particle, agglomerated particle radius=0.4 μ, 10.0 μ

Volume concentration of basic particle, agglomerated particle=3.9%, 10.8%

Default values of the unit settling distance were 2.5 μm

No. of compartments=1, 10

Total number of movements=100 and 1,000 for 403 and 4,030 particles, respectively.

In the case of particle settling with relaxation, particles were allowed to relax 5 times by 5 degrees in a random direction. Relaxation more than this amount did not show much change in sediment density by previous study. Simple settling of particles without relaxation showed a low density sediment occupying about 4/5 of the compartment height as shown in Fig. 3. Fig. 3(a) is the one compartment settling and Fig. 3(b) is the 10 compartments settling arranged in a vertical direction. Settling of particles with relaxation resulted in a dense sediment in Fig. 3(a) and (b). This was in good agreement with the corresponding experimental results reported by Schilling

*et al.*<sup>11)</sup> The settled layer can be divided into four regions after settling. The upper region is empty of particles (region 1 in Fig. 3). The second region is a transition zone (region 2 in Fig. 3) which shows a steep increase in the volume density. This surface layer is rough and has many vacant sites available for additional particles. The third is a region of constant density (region 3 in Fig. 3) where particles are sediment. The last is an interfacial region between the settled particles and the bottom of the box (region 4 in Fig. 3) where settling density was quite higher than inside the region of constant density due to the nature of the 2-dimensional settling (the particles were settled onto a geometrically flat plane.). The density profiles in Fig. 3 show the difference between layers settled with and without relaxation; these correspond to Schilling and Aksay's results<sup>11)</sup> for layers of freshly settled (no relaxation) and aged (relaxation). This suggests that the transition from an "attached-particle network" to the "compressed network" (in their terminology) depends on the relaxation. Even though the number of compartments and particles increased 10 times with same solid volume concentration, Fig. 3(b) shows basically the same volume density distribution. This proves that our model can be applied to bigger particle system.

Sediment strength was estimated on the planes with various orientations. Sediment strength and/or fracture energy is important to subsequent processing.<sup>11)</sup> Strength was estimated using the following formula.

$$\text{Sediment Strength} = \frac{\text{Bonding Energy per Contact} \times \text{No. of Bonds Crossing Plane}}{\text{Area of Plane} \times 2}$$

where bonding energy is the interparticle potential energy between two particle and was fixed at 100 kT for convenience in this paper.

Fracture energy depends on the direction at the bottom of the box which is shown in Fig. 4. The fracture energy is a maximum in the vertical direction at the bottom of the sediment. Relaxed particles showed a higher and more isotropic fracture energy than those of the not relaxed as shown in Fig. 4. This was because particles formed more bonds with neighboring particles after re-

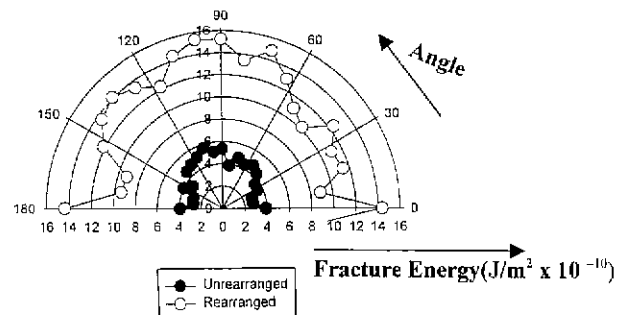


**Fig. 4.** Radial change in fracture energy of relaxed and unrelaxed particles measured at the bottom of the packed bed (radius=2.5 μm and energy unit=J/m² × 10<sup>-10</sup>).

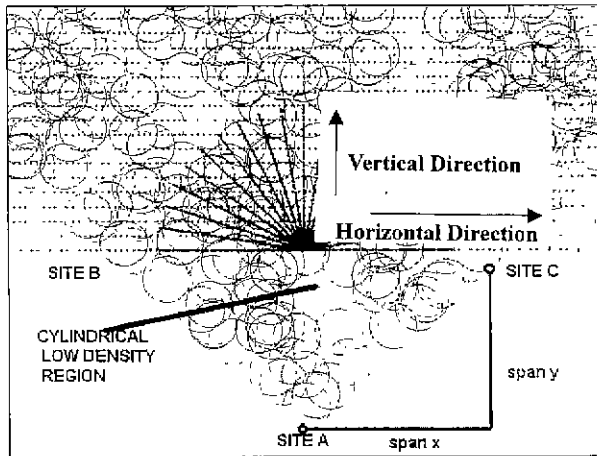


**Fig. 5.** Projection of packed particles with vertical and horizontal planes for fracture energy calculation in a tilted box.

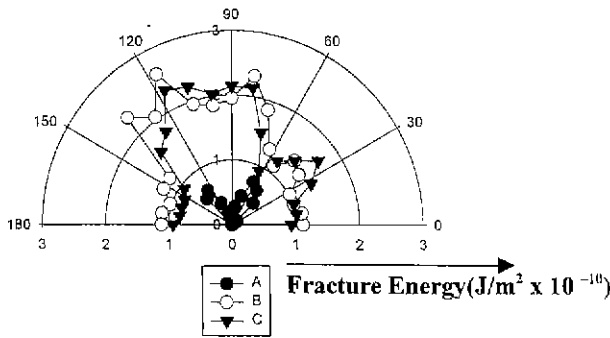


**Fig. 6.** Radial change in fracture energy of unrelaxed particles measured at the different locations in different box shapes. (span  $x=2.0$ , span  $y=2.0$ , radius= $2.0$  and energy unit= $J/m^2 \times 10^{-10}$ ).

laxation. Relaxation also caused strength to increase and to become more isotropic.

Different shapes were used to see how angular fracture energy depended on the settling direction and box geometry in Fig. 5. Radial anisotropic distributions of the fracture energy were measured at three different locations as shown in Fig. 5. Fracture energies at side location B and C clearly showed the maxima in the settling direction in the case of unrelaxed particles as shown in Fig. 6. The maxima shifted towards the normal to the box sides after relaxation as shown in Fig. 7. A minimum at location C appeared in the settling direction in both relaxed and unrelaxed cases; this was mainly due to the low fracture energy region at the corner of the box. There were several cylindrically shaped low fracture energy regions in addition to the one at the corner in the particle sediment in Fig. 5. The settling of particles in a corner caused bridge formation and resultant low fracture energy regions in the particle sediment. The same measurements were done in the case of lower degree of tilt; the results were similar as shown in Fig. 7 except that the fracture energy at location A was larger. This

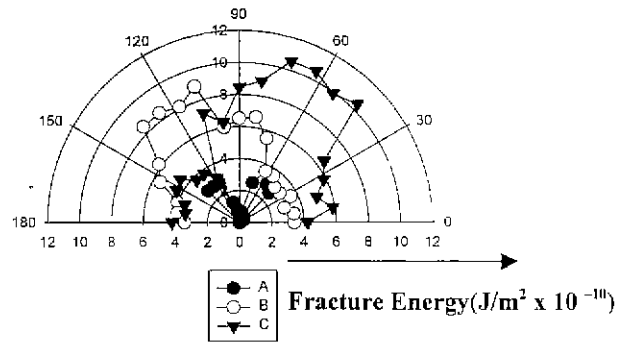


**Fig. 7.** Radial change in fracture energy of relaxed particles measured at the different locations in different box shapes. (span  $x=2.0$ , span  $y=2.0$ , radius= $2.0$  and energy unit= $J/m^2 \times 10^{-10}$ ).

was because there is less bridging between particles during settling.

### 4. Conclusions

A new three-dimensional settling algorithm was developed which incorporated metastable states. Full relaxation increased the settling density by about 50% and tripled the fracture energy compared to settling without relaxation, which was in quite good agreement with experimental results. There was a radial anisotropy of fracture energy in most sediments of unrelaxed particles and the fracture energy became more isotropic with relaxation. The changes in orientation of fracture energy maxima in a tilted box are explained by the change in particle network structure. Particles settled at the corner of a tilted box exhibit the bridging and low fracture energy regions in the particle sediment due to geometrical constraints caused by the corner. Such low fracture energy regions are probably unavoidable if the radius of curvature of an acute corner is comparable to particle radius.

### References

1. K. E. Davis and W. B. Russel, "A Model of Crystal Growth in the Sedimentation and Ultrafiltration of Colloidal Hard Spheres," *Adv. Ceram.*, **21**, 573-585 (1987).
2. R. Buscall, "The Sedimentation of Concentrated Colloidal Suspensions," *J. Colloids and Surfaces*, **43**, 33-53 (1990).
3. A. S. Michaels and J. C. Bolger, "Settling Rates and Sediment Volumes of Flocculated Kaolin Suspensions," *Ind. Eng. Chem. Fund.*, **1**, 24-33 (1962).
4. F. M. Tiller and Z. Khatib, "The Theory of Sediment Volumes of Compressible, Particulate Structures," *J. Colloid and Interface Science*, **100**(1), 55-67 (1984).
5. R. Buscall, P. D. A. Mills, J. W. Goodwin and D. W. Lawson, "Scaling Behavior of the Rheology of Aggregate Networks Formed from Colloidal Particles," *J. Chem. Soc. Faraday Trans. 1*, **84**(12), 4249-4260 (1988).
6. S. Warr and L. V. Woodcock, "Solid/Fluid Interfaces in

- Non-linear Steady States," *Faraday Discuss.*, **95**, 329-346 (1993).
7. M. J. Vold, "Computer Simulation of Floc Formation in a Colloidal Suspension," *J. of Colloid Science*, **18**, 684-695 (1963).
  8. J. C. Kim and D. M. Martin, "Computer Simulation of Three Dimensional Particle Packing," *J. of Kor. Ceram. Soc.*, **34**(9), 979-985 (1997).
  9. R. M. German, "Structure and Properties of Agglomerates"; pp. 55-88 in *Particle Packing Characteristics*, Metal Powder Ind. Fed., Princeton, New Jersey, 1989.
  10. N. D. Aparicio and A. C. F. Cocks, "On the Representation of Random Packings of Spheres for Sintering Simulations," *Acta. Metall. Mater.* **43**(10), 3873-3884 (1995).
  11. C. H. Schilling and I. A. Aksay, "Gamma-Ray Attenuation Analysis of Packing Structure Evolution During Powder Consolidation"; pp. 800-808 in *Ceramic Transactions, Vol. 1, Ceramic Powder Science II*. Ed. by G. L. Messing, E. R. Fuller, Jr. and H. Hausner. American Ceramic Society, Westerville, OH, 1988.
  12. J. C. Kim, "Computer Simulation of Colloidal Powder Processing," Ph.D. Thesis, Ames, Iowa, 1997.